Dependence of resistivity on electron density and temperature in graphene

W. Xu,[1,*] F. M. Peeters,[2] and T. C. Lu[3]
[1]*Department of Physics, Yunnan University, Kunming 650091, China*
[2]*Department of Physics, University of Antwerp, Groenenborgerlaan 171, B-2020 Antwerpen, Belgium*
[3]*Department of Physics, Sichuan University, Chengdu 610064, China*
(Received 13 October 2008; revised manuscript received 12 December 2008; published 11 February 2009)

On the basis of the momentum-balance equation derived from the Boltzmann equation in which electron interactions with impurities and acoustic and optic phonons are included, we examine the dependence of the resistivity in graphene on temperature and electron density. Simple analytical expressions for the different contributions to the resistivity are obtained. Our results reproduce recent experimental findings and we are able to understand the different temperature dependence of the resistivity for low and high density samples.

DOI: 10.1103/PhysRevB.79.073403 PACS number(s): 73.63.Hs, 72.15.Lh, 71.70.Ej

The realization of graphene-based electronic devices is an important scientific breakthrough.[1] Owing to its unique electronic band structure and the corresponding quasirelativistic features, graphene has high electronic mobility at relatively high temperatures up to room temperature. One of the major advantages of a graphene device is that the carrier density in the graphene layer can be controlled very effectively through a gate voltage.[1] Hence, graphene has been proposed as a building block for advanced electronic devices[2] such as graphene *p*-*n* and *p*-*n*-*p* junctions,[3,4] transistors,[5] etc. In recent years, the study of electronic transport properties of Dirac quasiparticles in graphene has rapidly become an important research topic in condensed-matter physics and nanoelectronics,[6] because this study is the basis for the application of graphene in advanced electronic devices.[7] In particular, very recently experimental work[8] has been carried out in examining the dependence of the resistivity in graphene on temperature and gate voltage (or electron density). It has been found experimentally[8] that the resistivity of graphene samples with different electron densities depends differently on temperature. Motivated by these important experimental works and interesting experimental findings, here we present a detailed theoretical study which is able to reproduce and to understand the different temperature dependence of low- and high-density graphene samples.

Recently, we developed a simple theoretical approach to study the quantum and transport conductivities in graphene at low temperatures where the electron-impurity (e-i) scattering is the principal channel to limit the transport properties of a graphene device.[9] This approach is based on the momentum-balance equation derived from the Boltzmann equation. By including electron interaction with only the charged impurities, we could calculate the transport coefficients as a function of carrier density at low temperatures and the obtained theoretical results were in line with those measured experimentally. In the present study, we generalize this approach to the case where the electron-phonon (e-p) interaction is also present in the graphene system. Thus, we can look into the electronic transport properties in graphene at relatively high temperatures. Here we consider a graphene sheet in the *xy* plane placed on top of a SiO_2 wafer, similar to the sample devices used in the experiments.[8] A carrier (electron or hole) in graphene can be described by Weyl's equation for a massless neutrino[10] and the wave function and energy spectrum for a carrier in the π bands near the K point can be obtained analytically.[10] We consider the conducting carriers in graphene to be electrons (i.e., in the presence of the positive gate voltages) and take e-i and e-p interactions as perturbations. For simplicity, we consider the charged impurities with effective concentration n_I to be located in the SiO_2 substrate close to the interface between the graphene and the substrate. This approximation has resulted in a good agreement between the theoretical results and the experimental data at low temperatures.[9] The electron interaction with acoustic phonons in graphene is mainly through the deformation potential coupling.[11] Moreover, we employ a valence-force-field model to describe the electron interaction with long-wavelength optic phonons in a graphene device.[12] Very recently Mariani and von Oppen[13] pointed out that the electron–flexural-phonon scattering plays an important role to determine the resistivity ρ in *free-standing* graphene below a crossover temperature $T_x \sim 70$ K via a relation $\rho \sim T^{5/2} \ln T$. In this study we are interested in a device system in which the graphene sheet is placed on a SiO_2 wafer. For such a graphene device, the electron density is much higher than that in a free-standing graphene, which implies that at low temperatures the resistivity is mainly determined by the e-i scattering in contrast to the case of a free-standing graphene. Moreover, for a graphene placed on a dielectric wafer the deformation potential interaction is enhanced due to the presence of the strain around the interface between the graphene sheet and the wafer material. Therefore we neglect the contribution from flexural-phonon scattering in the present study.

We employ a semiclassical Boltzmann equation as the governing transport equation to calculate the transport coefficients in graphene. When a driving dc electric field F_x is applied along the x direction of the system, the Boltzmann equation is

$$-\lambda \frac{eF_x}{\hbar} \frac{\partial f_\lambda(\mathbf{k})}{\partial k_x} = g_s g_v \sum_{\mathbf{k}',\lambda'} [F_{\lambda'\lambda}(\mathbf{k}',\mathbf{k}) - F_{\lambda\lambda'}(\mathbf{k},\mathbf{k}')], \quad (1)$$

where $f_\lambda(\mathbf{k})$ is the momentum-distribution function for a carrier in a state $|\mathbf{k},\lambda\rangle$, $\mathbf{k}=(k_x,k_y)$ is the carrier wave vector, $\lambda=+1$ refers to an electron and $\lambda=-1$ refers to a hole, $g_s=2$ and $g_v=2$ count for spin and valley degeneracies, and

 ©2009 The American Physical Society

$F_{\lambda\lambda'}(\mathbf{k},\mathbf{k}')=f_\lambda(\mathbf{k})W_{\lambda\lambda'}(\mathbf{k},\mathbf{k}')$ with $W_{\lambda\lambda'}(\mathbf{k},\mathbf{k}')$ being the electronic transition rate induced by electron interactions with impurities and phonons. $W_{\lambda\lambda'}(\mathbf{k},\mathbf{k}')$ measures the probability for scattering of a carrier from a state $|\mathbf{k},\lambda\rangle$ to a state $|\mathbf{k}',\lambda'\rangle$, which can often be obtained by using Fermi's golden rule. We employ the usual balance-equation approach[14] to calculate the transport coefficients. For the first moment, the momentum-balance equation[9] can be derived by multiplying $g_s g_v \Sigma_{\mathbf{k},\lambda} k_x$ on both sides of the Boltzmann equation, which reads

$$eF_x n_e = 16\hbar \sum_{\mathbf{k}',\mathbf{k},\lambda',\lambda} (k_x' - k_x) f_\lambda(\mathbf{k}) W_{\lambda\lambda'}(\mathbf{k},\mathbf{k}') \quad (2)$$

with n_e being the electron density. We assume that $f_\lambda(\mathbf{k})$ for a carrier can be described by a statistic energy distribution such as the Fermi-Dirac function in which the momentum is drifted by v_x, the drift velocity of the carrier, due to the presence of the driving field F_x.[14] Considering a weak driving electric field F_x, so that the condition $k_F v_x/v_F \ll k_x$ is satisfied, we have, for electron

$$f_+(\mathbf{k}) \simeq f(E_+(\mathbf{k})) - \hbar k_F v_x (k_x/k) f'(X)|_{X=E_+(\mathbf{k})} \quad (3)$$

and for hole $f_-(\mathbf{k}) \simeq 1$. Here, $k_F=\sqrt{\pi n_e}$ and $v_F=10^8$ cm/s are, respectively, the Fermi wave vector and Fermi velocity for an electron in graphene, $f(x)=[e^{(x-\mu^*)/k_BT}+1]^{-1}$ with μ^* being the chemical potential, $f'(x)=df(x)/dx$, and $E_\lambda(\mathbf{k})=\lambda\gamma k$ with $\gamma=\hbar v_F$ is the energy spectrum for a carrier in graphene. The result shown in Eq. (3) is equivalent to the relaxation time approximation on the basis of the Boltzmann equation.[15] By introducing Eq. (3) into Eq. (2) and by the definition $R=F_x/n_e e v_x$, the ohmic resistivity in graphene at finite temperature is obtained as

$$R = -\frac{R_0}{E_F^3}\int_0^\infty dE\, \Theta(E')E'E^2 R(E)\frac{df(E)}{dE}, \quad (4)$$

where $R_0=h/e^2$, $E_F=\gamma k_F$ is the Fermi energy, E is the electron energy, $E'=E$ for impurity scattering, and $E'=E+\hbar\omega_q$ and $E'=E-\hbar\omega_q$ for, respectively, phonon absorption and emission scattering with ω_q being the phonon frequency. Furthermore,

$$R(E) = \frac{2}{\pi\gamma^2}\sum_\nu \int_0^\pi d\theta [1-(E'/E)\cos\theta]|U_\nu(q,\theta)|^2$$

with $q=\sqrt{E'^2+E^2-2E'E\cos\theta}/\gamma$. We find that the interband transition contributes very weakly to the resistivity. The square of the matrix element for electron-impurity scattering is

$$|U_{\rm im}(q,\theta)|^2 = n_I\left(\frac{2\pi e^2}{\kappa}\right)^2\frac{1+\cos\theta}{2(q+K_s)^2},$$

where K_s is the inverse screening length induced by electron-electron (e-e) interaction[9] and κ is the dielectric constant for impurities in the SiO_2 wafer. For electron–acoustic-phonon scattering,

$$|U_{\rm ap}(q,\theta)|^2 = \begin{bmatrix} N_q \\ N_q+1 \end{bmatrix}\frac{\hbar E_D^2 q}{4\rho}\left(\frac{1}{v_l}+\frac{1}{v_t}\right)(1+\cos\theta),$$

where the upper (lower) case refers to phonon absorption (emission), the longitudinal and transverse acoustic-phonon modes are included, $N_q=(e^{\hbar\omega_q/k_BT}-1)^{-1}$ is the acoustic-phonon occupation number, $E_D=9$ eV is the deformation potential constant,[11] $\rho=6.5\times10^{-8}$ g/cm^2 is the areal density of the graphene sheet, and $v_l=2.1\times10^6$ cm/s and $v_t=7.0\times10^5$ cm/s are, respectively, the longitudinal and transverse sound velocities in the graphene layer.[8] The square of the matrix element for electron–optic-phonon scattering is

$$|U_{\rm op}(q,\theta)|^2 = \begin{bmatrix} N_0 \\ N_0+1 \end{bmatrix} g^2\gamma^2,$$

where the upper (lower) case refers again to phonon absorption (emission), the interactions with both longitudinal and transverse optic-phonon modes are included, $N_0=(e^{\hbar\omega_0/k_BT}-1)^{-1}$ is the optic-phonon occupation number, $\hbar\omega_0=196$ meV is the optic-phonon energy at the Γ point, and $g=\hbar(\mathcal{B}/b^2)/\sqrt{2\rho\hbar\omega_0}$ with $\mathcal{B}\sim 2$ and $b=a/\sqrt{3}$ being the equilibrium bond length with $a=1.42$ Å. We note that for electron–optic-phonon coupling, the terms with scattering and phonon angles induced by the longitudinal and transverse couplings[12] are canceled out. Using the momentum-balance equation derived from the Boltzmann equation, the average of the finite-temperature resistivity for graphene (which has a linear dispersion $E\sim k$), given by Eq. (4), differs significantly from the often used averages[16,17] such as $[\langle 1/\tau\rangle,\langle\tau\rangle]\sim\int dE\, E[-df(E)/dE][1/\tau(E),\tau(E)]$.

It can be shown that the strongest effect of the e-e screening on the e-i scattering is at $q\to 0$. Under the usual random-phase approximation (RPA),[16] $\lim_{q\to 0} K_s \simeq 4e^2\sqrt{\pi n_e}/\kappa_1\gamma$ with κ_1 being the dielectric constant for electrons in graphene. Considering an air-graphene-substrate system with the mismatch of the dielectric constants at the interfaces, we can evaluate κ and κ_1 from the bare dielectric constants for air, graphene, and the SiO_2 wafer using the mirror image method. We thus obtain $\kappa\simeq 4.25$ and $\kappa_1\simeq 2.5$. For electron–acoustic-phonon coupling at relatively high temperatures, so that $\hbar\omega_q \ll k_BT$ and $\hbar\omega_q \ll \gamma k$, the scattering is quasielastic.[18] In graphene, the optic-phonon energy $\hbar\omega_0=196$ meV or 2275 K is much higher than room temperature. Furthermore, for a typical graphene sample, the electron density $n_e\sim 10^{12}$ cm^{-2}, so that the Fermi energy or temperature $E_F=\gamma\sqrt{\pi n_e}\sim 1345$ K is about four times larger than room temperature. Taking these features into consideration, up to room temperature the chemical potential $\mu^*\simeq E_F-(\pi k_BT)^2/6E_F$ and the contributions from different scattering mechanisms to resistivity are obtained approximately as

$$R_{\rm im} \simeq R_0(1.302/\kappa^2)(n_I/n_e)[1+(\pi k_BT/E_F)^2/2], \quad (5)$$

which depends on $(n_I/n_e)(1+\alpha T^2/n_e)$ with $\alpha=\pi k_B^2/2\gamma^2$,

$$R_{\rm ap} \simeq R_0\frac{E_D^2 k_BT}{2\gamma^2\rho}\left(\frac{1}{v_l^2}+\frac{1}{v_t^2}\right)[1+(\pi k_BT/E_F)^2/2], \quad (6)$$

which depends on $T(1+\alpha T^2/n_e)$, and

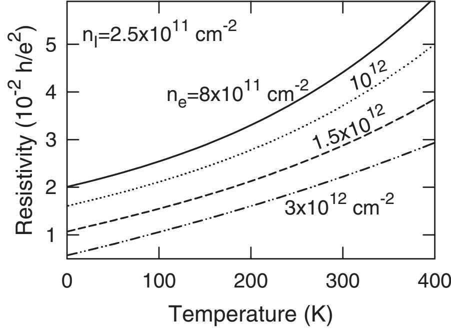

FIG. 1. Temperature dependence of the resistivity for fixed impurity concentration n_I and different electron densities n_e.

$$R_{\mathrm{op}} = R_0(2g^2)[N_0 I_1 + (N_0+1)I_2], \qquad (7)$$

which depends strongly on temperature and electron density, where $I_1 = 1 + \hbar\omega_0/E_F + (\pi k_B T/E_F)^2/2$ and

$$I_2 = (\hbar\omega_0/E_F)^3 \int_0^\infty dx\, f((x+1)\hbar\omega_0)(3x^2+4x+1).$$

In Eqs. (5)–(7) we have obtained the rather simple expressions for resistivity induced by different scattering mechanisms. The total resistivity then is

$$R = R_{\mathrm{im}} + R_{\mathrm{ap}} + R_{\mathrm{op}}. \qquad (8)$$

In our calculation the effective impurity concentration n_I is the only fitting parameter needed for evaluating the resistivity.

In Fig. 1 we show the resistivity as a function of temperature at a fixed impurity concentration n_I for different electron densities n_e. For low-density samples (e.g., $n_e=8\times10^{11}$ cm^{-2}) the resistivity does not depend linearly on temperature, whereas for high-density samples (e.g., $n_e=3\times10^{12}$ cm^{-2}) a rough $R\sim T$ relation can be observed. As one can see, the results shown in Fig. 1 agree both qualitatively and quantitatively with those measured experimentally.[8] In order to understand why ρ in graphene depends differently on T for samples with different n_e, we show in Fig. 2 the contributions from the different scattering mechanisms to the resistivity. We find that for a low-density sample (e.g., $n_e=8\times10^{11}$ cm^{-2}), the e-i interaction is the major scattering channel over a wider temperature range up to 300 K. Because $R_{\mathrm{im}}\sim(1+\alpha T^2/n_e)$, the behavior $R\sim T^2$ can be more easily observed for low-density samples. In contrast, for high-density samples (e.g., $n_e=3\times10^{12}$ cm^{-2}) the electron–acoustic-phonon scattering becomes significant when $T>50$ K. Because $R_{\mathrm{ap}}\sim T(1+\alpha T^2/n_e)$, the behavior $R\sim T$ is more pronounced for high-density samples. From Fig. 2, we see that, in graphene, the acoustic-phonon scattering depends weakly on the electron density up to room temperature and the optic-phonon scattering increases rapidly with temperature for high temperatures.

In Fig. 3, the total resistivity and those induced by different scattering mechanisms are shown as a function of electron density at a fixed impurity concentration for different temperatures. When $n_e<6\times10^{11}$ cm^{-2}, the resistivity is mainly limited by impurity scattering and, therefore, R

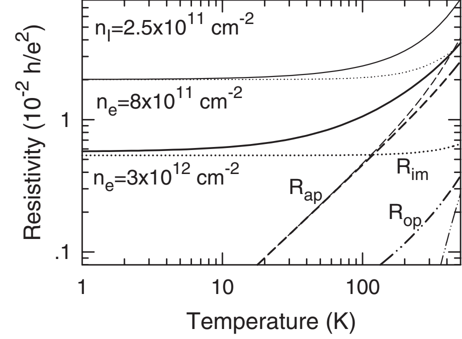

FIG. 2. Contributions from different scattering mechanisms to resistivity at a fixed impurity concentration n_I for different electron densities $n_e=8\times10^{11}$ cm^{-2} (thinner curves) and $n_e=3\times10^{12}$ cm^{-2} (thicker curves). Here R_{im}, R_{ap}, and R_{op} are resistivities induced by scattering with, respectively, impurities, acoustic phonons, and optic phonons. The total resistivities are shown as solid curves.

$\sim 1/n_e$. This is a well-known result observed both experimentally and theoretically.[9,16] The electron–optic-phonon scattering increases rapidly with electron density. At high temperatures (e.g., $T=300$ K) the acoustic-phonon coupling is the main scattering channel to determine the resistivity in high-density samples, whereas at low temperatures (e.g., $T=30$ K) the optic-phonon scattering is the major mechanism responsible for the resistivity in high-density samples. These features are in sharp contrast to those observed in III-V-based two-dimensional electron gas (2DEG) systems. It is known both experimentally and theoretically[19] that in III-V-based 2DEGs: (i) The electron-impurity scattering dominates the resistivity when $T<10$ K. ρ_{im} depends strongly on n_e but very weakly on T. (ii) The electron–acoustic-phonon scattering is responsible for resistivity when $10<T<50$ K. $\rho_{\mathrm{ac}}\sim T\sim 1/n_e$. (iii) The electron–optic-phonon coupling determines the resistivity when $T>50$ K, where ρ_{op} depends strongly on T but very weakly on n_e. As a result, in GaAs-based 2DEGs the resistivity at $T>50$ K depends very weakly on sample parameters such as n_e and the width of the quantum well layer. In contrast, in graphene the temperature dependence of the resistivity depends on the electron density of the sample and vice versa.

It should be noted that, in this study, we have considered

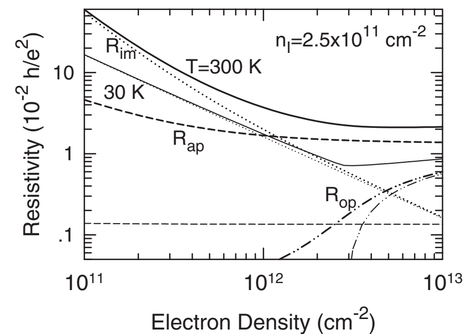

FIG. 3. Resistivity as a function of electron density at a fixed impurity concentration n_I for two different temperatures $T=300$ K (thicker curves) and $T=30$ K (thinner curves).

a relatively high-density graphene system realized by placing the graphene sheet on the dielectric substrate in conjunction with the published experimental work.[8] In high-density graphene samples the Fermi level ($E_F = \gamma\sqrt{\pi n_e}$) is far from the Dirac point $E=0$. Because the transport properties are determined mainly by electronic transition around the Fermi level [see Eq. (4)], the nonlinear features around the Dirac point affect weakly the transport coefficients such as the resistivity. Moreover, for high-density samples we can use the RPA approximation[16] to count the effect of e-e screening. As a result, the simple approach developed here cannot be applied to the low-density samples in which the effect of correlation becomes important, where the interaction parameter $\gamma_s \gg 1$.

In this study, we have developed a simple approach to examine the resistivity induced by electronic scattering with impurities and acoustic and optic phonons in graphene that is placed on top of a SiO_2 wafer. The resistivity has been calculated by using only one fitting parameter n_I (the effective impurity concentration) and quantitative agreement with recent experimental results[8] can be achieved. The obtained theoretical results have been presented by simple analytical expressions and can be used to understand and to reproduce the experimental findings. We have confirmed that the dependence of the resistivity on electron density and temperature in graphene differs significantly from that in III-V-based 2DEG systems.

This work was supported by the Department of Science and Technology of Yunnan Province, China; the Ministry of Education, China; and by the Flemish Science Foundation (FWO-Vl).

*wenxu_issp@yahoo.cn

[1] K. S. Novoselov, A. K. Geim, S. V. Morozov, D. Jiang, M. I. Katsnelson, I. V. Grigoreva, S. V. Dubonos, and A. A. Firsov, Nature (London) **438**, 197 (2005); Y. B. Zhang, Y. W. Tan, H. L. Stormer, and P. Kim, *ibid.* **438**, 201 (2005); N. Tombros, C. Jozsa, M. Popinciuc, H. T. Jonkman, and B. J. Van Wees, *ibid.* **448**, 571 (2007).

[2] For a review, see, e.g., A. K. Geim and A. H. MacDonald, Phys. Today **60**(8), 35 (2007).

[3] J. R. Williams, L. C. DiCarlo, and C. M. Marcus, Science **317**, 638 (2007).

[4] B. Özyilmaz, P. Jarillo-Herrero, D. Efetov, D. A. Abanin, L. S. Levitov, and P. Kim, Phys. Rev. Lett. **99**, 166804 (2007).

[5] A. K. Geim and K. S. Novoselov, Nature Mater. **6**, 183 (2007).

[6] See, e.g., *The Special Issue on Graphene*, edited by S. Das Sarma, A. K. Geim, P. Kim, and A. H. MacDonald, Solid State Commun. **143**, 1 (2007).

[7] M. C. Lemme, T. J. Echtermeyer, M. Baus, and H. Kurz, IEEE Electron Device Lett. **28**, 282 (2007).

[8] J. H. Chen, C. Jang, S. Xiao, M. Ishigami, and M. S. Fuhrer, Nat. Nanotechnol. **3**, 206 (2008).

[9] H. M. Dong, W. Xu, Z. Zeng, T. C. Lu, and F. M. Peeters, Phys. Rev. B **77**, 235402 (2008).

[10] J. W. McClure, Phys. Rev. **104**, 666 (1956).

[11] T. Stauber, N. M. R. Peres, and F. Guinea, Phys. Rev. B **76**, 205423 (2007).

[12] T. Ando, J. Phys. Soc. Jpn. **76**, 024712 (2007).

[13] E. Mariani and F. von Oppen, Phys. Rev. Lett. **100**, 076801 (2008).

[14] W. Xu, Phys. Rev. B **71**, 245304 (2005); W. Xu, F. M. Peeters, and J. T. Devreese, *ibid.* **43**, 14134 (1991).

[15] See, e.g., K. Seeger, *Semiconductor Physics*, Springer Series in Solid-State Sciences Vol. 40 (Springer, New York, 1982).

[16] E. H. Hwang, S. Adam, and S. Das Sarma, Phys. Rev. Lett. **98**, 186806 (2007).

[17] F. T. Vasko and V. Ryzhii, Phys. Rev. B **76**, 233404 (2007).

[18] C. Jacoboni and L. Reggiani, Rev. Mod. Phys. **55**, 645 (1983).

[19] D. R. Leadley, R. J. Nicholas, W. Xu, F. M. Peeters, J. T. Devreese, J. Singleton, J. A. A. J. Perenboom, L. van Bockstal, F. Herlach, C. T. Foxon, and J. J. Harris, Phys. Rev. B **48**, 5457 (1993).